1968-06

The excitation of helium by high energy proton bombardment at various pressures.

Tullington, Bernard John Jr

Monterey, California. Naval Postgraduate School

UNITED STATES
NAVAL POSTGRADUATE SCHOOL

THESIS

THE EXCITATION OF HELIUM BY HIGH ENERGY PROTON BOMBARDMENT AT VARIOUS PRESSURES

by

Bernard John Tullington, Jr.

June 1968

THE EXCITATION OF HELIUM

BY HIGH ENERGY PROTON BOMBARDMENT

AT VARIOUS PRESSURES

by

Bernard John Tullington, Jr.
Major, United States Army
B.S., Military Academy, 1957

Submitted in partial fulfillment of the
requirements for the degree of

MASTER OF SCIENCE IN PHYSICS

from the

NAVAL POSTGRADUATE SCHOOL
June 1968

ABSTRACT

The intensities of several helium spectral lines are analyzed for their dependence on pressure. Neutral helium was bombarded by protons, accelerated in a Van de Graaff generator to energies of 1.6 MeV before they passed through an aluminum foil window into the collision chamber. Eight helium emission lines and one nitrogen line (impurity) were detected by photographic analysis of the collision spectrum at various pressures. Relative intensities of five of the helium emission lines were measured with photoelectric apparatus at pressures from 10^{-5} - 550 Torr. Lines of 6678Å, 7281Å, 7065Å and 5876Å show a similiar, but not exact, functional dependence on pressure. The 3889Å line appears to have a quite different pressure dependence that may possibly be due to the nitorgen impurity. Suggested experimental improvements are discussed.

TABLE OF CONTENTS

LIST OF ILLUSTRATIONS

ACKNOWLEDGEMENTS

The writer wishes to express his appreciation for the continuous assistance and encouragement given him by Professor E.A. Milne in this investigation, as well as to Professor R.L. Kelly for his assistance in the photographic and optical aspects of the apparatus; and to Mr. Ray Garcia who provided technical assistance in the maintenance of the electronic equipment and Van de Graaff accelerator.

This project was supported in part by funds provided by the Naval Ordnance Laboratory.

I. INTRODUCTION

The processes by which excited states of helium are formed by ion-atom impact have been the subject of an increasing number of studies. These studies have progressively extended the projectile energy range from earlier investigations of less than 200 keV to 1 MeV. While these investigations are of fundamental importance in determining excitation cross sections and are valuable in verifying theoretical predictions at high energies, they are based primarily on the simplifying assumption of the single hit condition.

The single hit condition assumes an excitation cross section independent of pressure and thus demands a very low target particle density. The normal experimental procedure (under this assumption) is to have the collision take place in a differentially pumped chamber under pressures in the region of 10^{-4} or 10^{-5} Torr. Emission cross sections (or apparent cross sections as they are sometimes called) are then measured over a limited pressure range. If the emission cross section is found not to be dependent on pressure, the single hit condition is assumed to be satisfied. If a pressure dependence is noted, as is often the case, the procedure has been either to operate in so called regions of non-dependence or to extrapolate the emission cross section to zero pressure and use that value.

The next step in better understanding the excitation process is obvious. If the single hit condition is not satisfied, what are the processes leading to the formation of the excited states of

helium? A starting point in answering this question is an understanding of the pressure dependence, if any, of the emission cross sections. Five helium spectral lines are observed as a function of pressure representing both para (singlet) and ortho (triplet) transitions.

II. BACKGROUND

Neutral Helium may be excited by proton bombardment by direct excitation;

$$H^+ + He = H^+ + He(n,l)$$

or by charge transfer;

$$H^+ + He = H + He^+(n,l)$$

or by simultaneous ionization and excitation;

$$H^+ + He = H^+ + He^+(n,l) + e^-$$

Once excited, He(n,l) may fall to a metastable state or ground state by radiative decay, or it may be de-excited by collisional transfer.

The rate of change of the population density of any state i may be written as:

$$\frac{dN_i}{dt} = nv N^-_i + \sum_{k>i} A_{ki} N_k - \sum_{j<i} A_{ij} N_i + C_i(n,N,V) \quad (1)$$

The first term on the right expresses the rate of collisional population in terms of projectile density (n), projectile velocity (v), target density N and the excitation cross section σ_i. The second term provides for population of the i^{th} state by cascade from all states k higher than i, in terms of the transition probability A_{ki} and the population density of state k, (N_k). The third term is a measure of the rate at which state i is depopulated by radiative decay from state i to all states j lower than i, also in terms of transition probability A_{ij} and state density N_i. The last term of equation (1) represents secondary processes such as collisional depopulation, collisional transfer and population by absorption of resonance photons. Gabriel and Heddle[3] have developed a

technique for determining the value of this function under single hit conditions by a method of simultaneous solutions. For brevity it is shown here simply as a possible function of n, v, and N.

For steady state conditions,

$$\frac{dN_i}{dt} = 0.$$

Equation 1 can be solved for σ_i and is

$$\sigma_i = \frac{1}{nvN} \left[\sum_{j<i} A_{ij} N_i - \sum_{k>i} A_{ki} N_k - C_i(n,v,N) \right]. \qquad (2)$$

The normal development[9] which follows is to define an emission cross section in terms of the number of photons emitted/sec/cm of beam path, J_{ij}, as

$$\sigma_{ij} = \frac{J_{ij}}{NI}, \qquad (3)$$

where N is the number density of the target, I = nv A, the number of incident projectiles per second, A the beam cross sectional area, and $J_{ij} = A_{ij} N_i A$.

Equation 3 is now

$$\sigma_{ij} = \frac{A_{ij} N_i}{Nnv}, \qquad (4)$$

the cross sectional area cancelling out.

Making the appropriate substitution, equation (2) now becomes

$$\sigma_i = \sum_{j<i} \sigma_{ij} - \sum_{k>i} \sigma_{ki} + C', \qquad (5)$$

where $C' = C(n,v,N)/nvN$.

For some specific state l (lower than i), the intensity of the emission i→l transition may be related to the total photon emission by all downward transitions by

$$\frac{J_{il}}{\sum_{j<i} J_{ij}} = \frac{A_{il}}{\sum_{j<i} A_{ij}} \qquad (6)$$

Relating equations (3) and (6) and substituting where appropriate into equation (5) yields;

$$\sigma_i = \frac{J_{il}}{A_{il}} \sum_{j<i} A_{ij} - \sum_{k>i} \sigma_{km} \frac{A_{ki}}{A_{km}} + C'. \qquad (7)$$

The second term on the right is the cascade correction and is written in terms of the state m to show all emission functions into i need not be measured. Any emission out of state m can be related to the total emission through the ratio of transition probabilities. This is fortunate, as the transition probabilities for helium are well known and have been tabulated by the Bureau of Standards[10].

It is now obvious that knowing J_{il} for only a few transitions will lead to the determination of the excitation cross section σ_i, providing C can be neglected.

The photoelectric apparatus will accept photons through a solid angle ω and will deliver a signal S_{ij} by the relationship

$$J_{ij} = \frac{4\pi}{\omega} \frac{S_{ij}}{L\, K(\lambda)} \qquad (8)$$

where L is the beam length and $K(\lambda)$ is a dimensionless factor which takes into account the systems detection sensitivity and losses due to refraction and reflection at optical surfaces.

$K(\lambda)$ may be determined by measuring the signal from a standard filament lamp under the same optical conditions the collision is observed. For the wavelength under consideration,

$$S_\lambda = K(\lambda)\, E_\lambda\, D_\lambda\, dw\, d\omega; \qquad (9)$$

where E_λ is the emissive power of the lamp at the wavelength of interest, D_λ the inverse dispersion of the spectrometer ($\mathring{A}$/mm), d the spectrometer exit slit width and ω the area viewed by the optical system. E_λ may be determined from the filament temperature which may be measured by a pyrometer if this information is not furnished by the manufacturer.

Solving (9) for $K(\lambda)$ and substituting into equation (8) yields,

$$I_{ij} = 4\pi \frac{S_{ij}}{S_\lambda} E_\lambda\, D_\lambda\, dw \qquad (10)$$

Thus, under single hit conditions, where σ_{il} is not a function of N, and C' can be ignored, the excitation cross section can readily be determined by measuring σ_{il}, as:

$$\sigma_{il} = 4\pi \left(\frac{S_{il}}{S_\lambda}\right) \frac{E_\lambda\, D_\lambda\, dw}{NI} \qquad (11)$$

It should be noted that neither the solid angle ω or the collision path length L need be measured under these conditions.

III. EXPERIMENTAL PROCEDURES

From section II, if σ_{il} is independent of pressure, equation (11) may be written as

$$P = C'' R \qquad (12)$$

where

$$C'' = \frac{4\pi E_o D_o dw N kT}{\sigma_{il} S_o V} .$$

$R = S_{il}/I$ is a measure of the photon emission intensity relative to the photon beam current which is measured by the optical apparatus. P, the target pressure, is related to the target density by the ideal gas law, PV = N kT.

A plot of Intensity versus Pressure should result in a straight line with a slope of C", if σ_{il} is independent of pressure.

THE HELIUM COLLISION SPECTRUM

The proton beam was produced by a 2 MeV Van de Graaff particle accelerator and mass analyzed by a magnet which bends the beam through an angle of 10^{o}. A thin aluminum foil, (about 1.6×10^{-3} cm) was used to separate the particle drift tube from the collision chamber. The collision chamber was constructed of pyrex and fitted with an aluminum faraday cup to measure the proton beam current. A 3.5 cm quartz lens, (f = 16.3 cm) was used to focus the collision spectrum on the optical apparatus. This apparatus is shown schematically in Fig. 1 and photographically in Fig. 15.

Mid way between the collision chamber and viewing lens is the vacuum manifold (below) and a gas control manifold (above). The vacuum system, consisting of a 2 inch oil diffusion pump, backed

up by a single fore pump, was capable of evacuating the chamber to 4×10^{-6} Torr. The control manifold provided 5 inlets into the collision chamber, (numbered in Fig. 1). The ports were used for: (1) gas inlet; (2) Wallace Tiernan, 1 to 50 Torr pressure gauge; (3) ion gauge; (4) fore pump; and (5) a mercury monometer.

The beam was viewed at 90° to the collision chamber by the optical apparatus.

To determine the purity of the target gas, the collision beam was photographed by a large Gaertner L254 Quartz spectrometer, shown schematically in Fig. 2. This spectrometer provides photographic coverage from 1900Å to 8000Å, on photographic plates 4 x 10 inches.

Numerous unsuccessful attempts were made to obtain a spectroscopically pure helium photograph. These attempts included water pumped commercial helium and vapor from liquid helium. These procedures led to spectrographs of primarily nitrogen and some other impurities but no helium lines were evident.

The most satisfactory procedure was to pump the system for several hours, saturate it with research grade helium and repump prior to a run.

Research grade helium (rated single impurities of 2 parts per million of neon by the manufacturer) was used and the tank was connected directly through a gas regulator to the inlet manifold. Even with this procedure a single Nitrogen line (3914Å) was still evident at pressures above 50 Torr.

Photographs were taken at pressures of 50 Torr, 100 Torr, 200 Torr, and 600 Torr with varying results. Beam currents of 2 to 2.5 microamps were common at an indicated particle energy of 1.65 MeV. Exposure times varied from 1.5 to 3 hours. In general, it was necessary to increase exposure times at lower pressures for satisfactory results.

It became evident that emission intensity would be the critical factor. Increasing the beam current does increase the intensity but currents of 3 microamps and higher result in very short life for the aluminum windows.

The photographs were made on Kodak emulsion I-N and 103F plates. Best results were obtained from the I-N which is designed for wavelengths up to 9000Å.

The lines identified from the plates are listed in Table I along with their corresponding transitions, and they are shown schematically on the energy-state diagram in Fig. 3.

Table I. Observed Helium Spectral Lines by Photographic Analysis

Wavelength	Transition
3888.65	$2^3S - 3^3P$
3964.73	$2^1S - 4^1P$
4471.48	$2^3P - 4^3D$
5025.68	$2^1S - 3^1P$
5875.62	$2^3P - 3^3D$
6678.15	$2^1P - 3^1D$
7065.19	$2^3P - 3^3S$
7281.35	$2^1P - 3^1S$

It should be noted that many of the optically allowed transitions fell outside the observable range of the optical equipment.

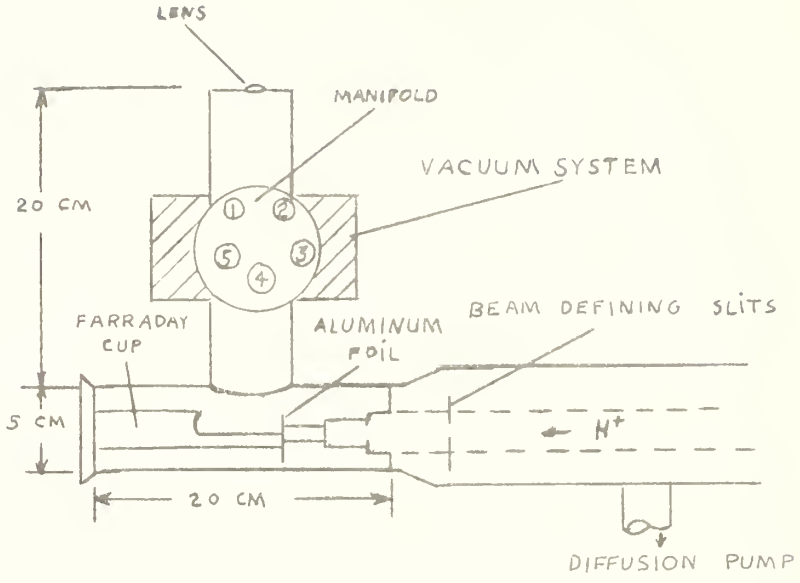

Figure 1. Top view of collision chamber showing the relative positions of the drift tube, vacuum system and control manifold

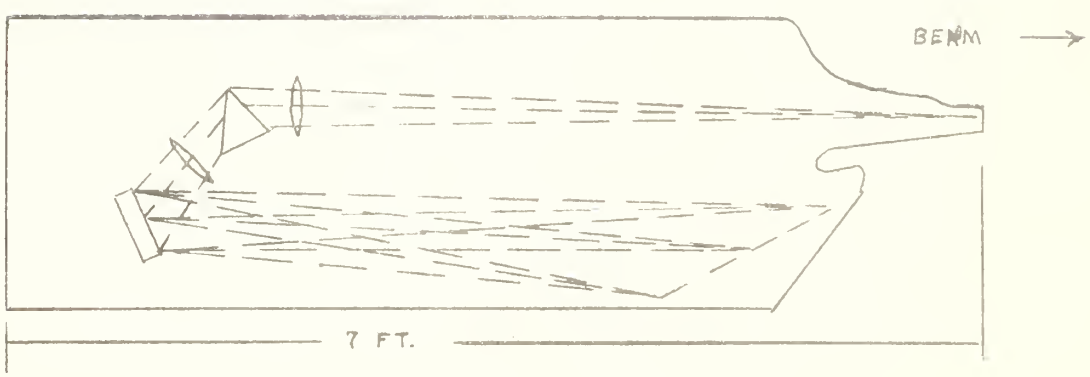

Figure 2. Schematic representation of the Gaertner L254 Quartz Spectrometer Optical System

INTENSITY VS PRESSURE

The helium gas was let in through a needle valve into the thoroughly evacuated collision chamber to a pressure of about 50 Torr. The beam was then admitted into the chamber. Light from the collision region was focused onto the entrance slit of a 0.25 meter Jarrel Ash monochrometer. The monochrometer is designed to select light of wavelengths from 1500Å to 9000Å ± 10Å. Due to low intensities, however, it was necessary to use wider slits which greatly reduced this resolving power. The monochrometer was manually set to pass the desired wavelength to a dry-ice-cooled PM 101-1 photomultiplier assembly. A 7102 photomultiplier tube was used and operated at 1250 volts (negative). The output current from the photomultiplier went to a current integrator where the total charge collected was recorded. The entire optical assembly was then covered with a black cloth to reduce the amount of stray light while the chamber was again evacuated. With the entrance slit covered, the beam was again turned on and the beam current integrator was allowed to accumulate 1500 microcoulombs. The time required for this collection and the total charge collected by the photomultiplier integrator were recorded. Figure 4 shows a schematic representation of the photoelectrical set-up. Figures 16, and 17 are photographs of the apparatus.

The charge thus collected divided by time was taken to be the dark current. This value multiplied by the time for subsequent readings was subtracted from the photomultiplier output.

The initial data were taken with the diffusion pump engaged and the entrance slit exposed. This was considered to be the zero pressure readings. The beam was turned on from the control console,

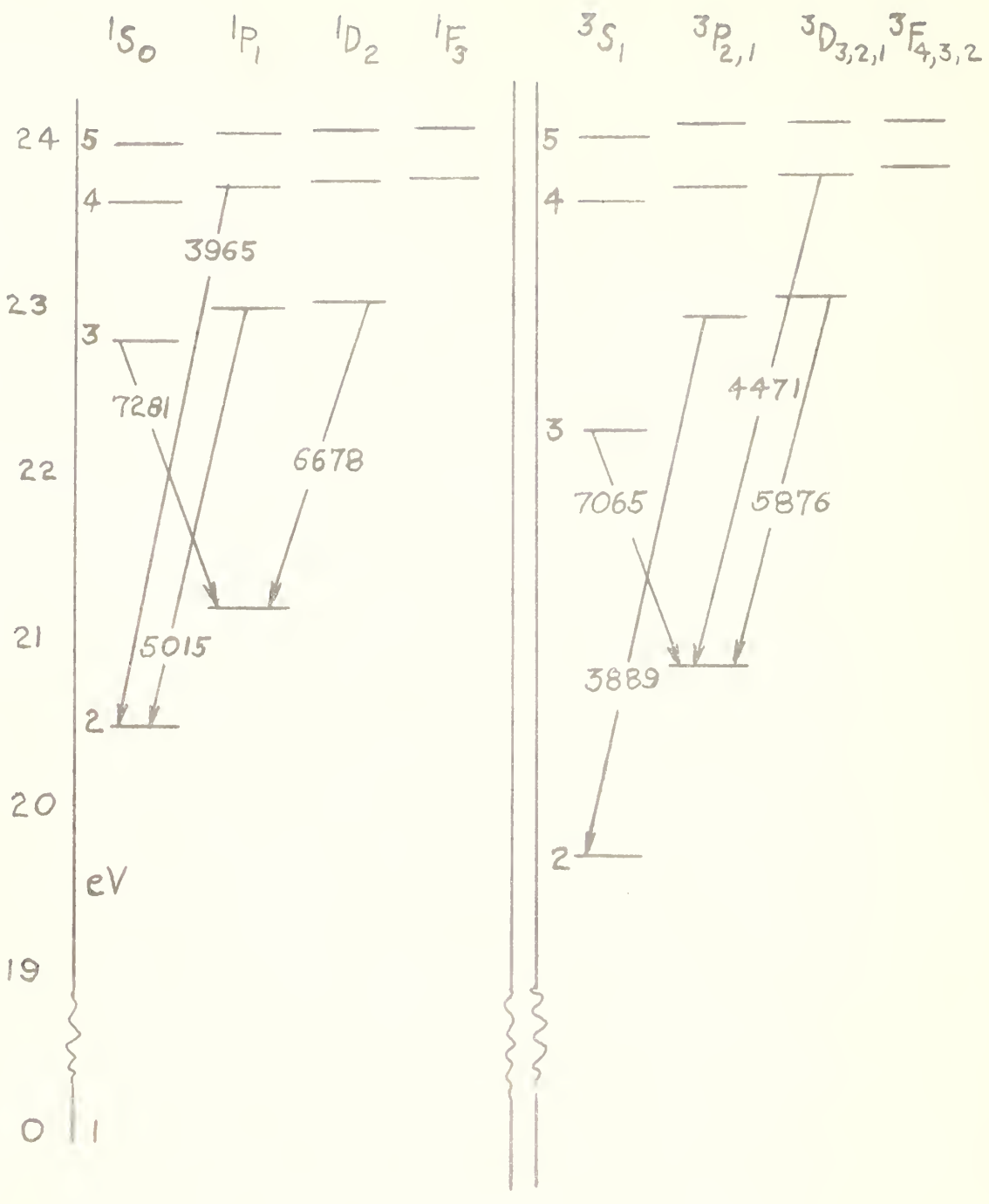

Figure 3. Energy-states diagram for photographically detected He spectrum lines by H^+ bombardment

(see Fig. 17). This automatically activated the timer, beam current integrator and photomultiplier current integrator. At each selected pressure the helium pressure, time, photomultiplier coulomb collection and beam coulomb collection were recorded. Pressure intervals of 1 or 2 Torr were initially selected up to 50 Torr, then various convenient intervals were selected up to a maximum pressure of 760 Torr. It was found that the intensity behavior remained constant after about 300 or 500 Torr. Subsequent runs were made at less frequent intervals to reduce the effect of the changing dark current. It was observed that the dark current would remain essentially constant over a time span of about 2 hours. After that, the dark current rose rapidly and could no longer be assumed constant. Repacking the photomultiplier assembly with dry ice did not alter this phenomenon. Cooling by liquid nitrogen vapor also proved to be unsuccessful in prolonging the effective time for a constant dark current.

From the data collected as described above, the transition intensity was computed as;

$$R = (Ph - DC \times t)/B; \qquad (13)$$

where Ph = charge collected via P.M. assembly, DC = dark current, t = time, and B = charge collected by the beam integrator.

Five lines observed by the photographic analysis were measured by this technique. It was impossible to study 3 of the lines due to the low intensities involved. It was even necessary to use wider slits than those provided in the monochrometer to study the five lines. The monochrometer has standard slits of .1 mm. The slits used were about .8 mm wide.

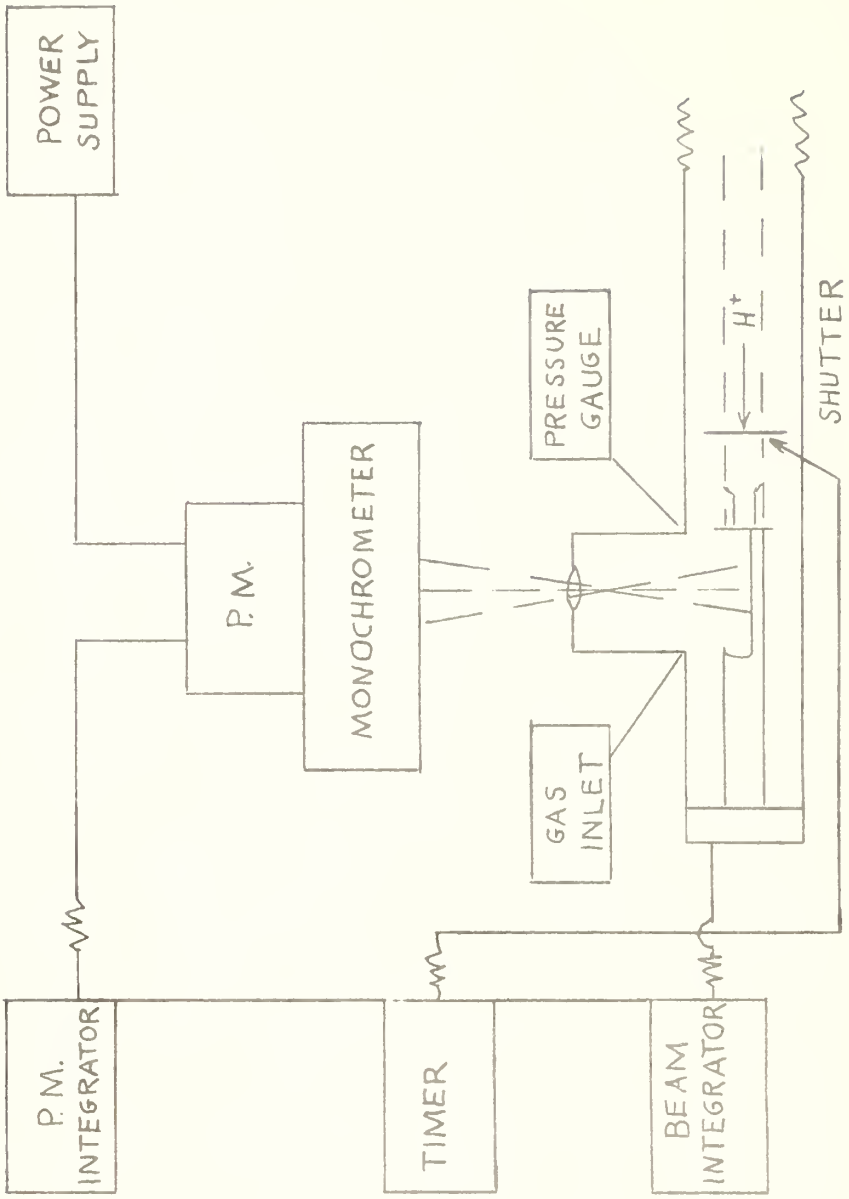

Figure 4. Schematic of optical apparatus for intensity vs. pressure measurements

IV. RESULTS AND CONCLUSIONS

Intensities as described above were measured vs pressure for the singlet lines; 6678Å ($2^1P - s^1D$) and 7281Å ($2^1P - 3^1S$), and the triplet lines; 3889Å ($2^3S - s^3P$), 5876Å ($2^3P - 3^3D$) and 7065Å ($2^3P - 3^3S$). A plot of intensity vs pressure for these lines is shown in Figs. 5, 6, 7, 8 and 9 respectively.

The singlet transition intensities appear to have a similar functional dependence on pressure that rapidly increases up to about 100 Torr where they undergo a levelling off effect. This is followed by a continuous general rise in intensity to the maximum pressures indicated.

The triplet transitions show no such functional similarity except for the 7065 line which is similar to the 2 singlet lines mentioned above. The 7065 line also rises rapidly during the first 100 Torr of pressure. The 3889 line has a slight sigmoidal tendency which suggests 2 influencing factors are possibly responsible for its peculiar behavior. The 5876 line indicates a very rapid rise in intensity, reaching its near maximum at about 25 Torr and then a slight general rise with pressure similar to the other lines.

It is obvious from these curves that there is, indeed, a functional dependence of the emission cross sections on pressure which is to be expected. The single hit condition is hardly expected to hold at these high pressures.

From equation 7,

$$\sigma_{il} \left[\tau_i + \sum_{k>i} \sigma_{km} \frac{A_{ki}}{A_{km}} - C'(N) \right] \frac{A_{il}}{\sum_{j<i} A_{ij}} \quad . \quad (14)$$

C' is now shown only as a function of N. In this experiment the velocity and projectile density were held relatively constant. In fact, for a given emission $i \rightarrow l$, all of the terms are constant except C'(N), and equation (14) may be written as;

$$\sigma_{il} = A - C'(N) \times \frac{A_{il}}{\sum_{j \neq i} A_{ij}} . \qquad (15)$$

Equation (12) may be written as;

$$\sigma_{il} = D \left(\frac{R}{P}\right) . \qquad (16)$$

A and D in equation (15) and (16) are constants. Since $N \propto P$, $C'(N) \propto C'(P)$. Equating (15) to (16) yields,

$$D\left(\frac{R}{P}\right) = A - C'(P) \times \frac{A_{il}}{\sum_{j \neq i} A_{ij}} . \qquad (17)$$

Substituting from equation (6) and multiplying both sides by P/R yields:

$$D = A \times \left(\frac{P}{R}\right) - C'(P) \times \frac{J_{il}}{\sum_{j \neq i} J_{ij}} \times \left(\frac{P}{R}\right) . \qquad (18)$$

From equation (10), $J_{il} \propto S_{il}$, and $R = S_{il}/I$, where I in this experiment is held constant. For any given emission, $\sum_{j \neq i} J_{ij}$ will either be a constant or a function of pressure, P. Equation (18) can now be written as,

$$D = A\left(\frac{P}{R}\right) - f(P) \times E, \text{ or}$$

$$\frac{P}{R} = f(P) \times E' + D', \qquad (19)$$

where $f(P)$ is some unknown function of pressure, and E' and D' are constants absorbing $\frac{I}{A}$.

The same data shown in Figs. 5, 6, 7, 8, and 9, were used to plot P/R vs P. If σ_{ij}, the quantity of interest, is singly dependent on pressure, P/R vs. P should plot as a straight line from equations (15) and (19).

Figures 10, 11, 12, 13, and 14 show the results of this manipulation.

The two singlet lines, 6678Å and 7281Å, again show a similar functional dependence. Although the sharp rise noted earlier has been smoothed out, there is still a slight bow in the curve.

The triplet lines show a slight uniformity. The 7065 line has an apparent curve up to about 40 Torr after which it is essentially linear. Conversely, the 5876 line is linear up to about 150 Torr, after which it exhibits a slightly decreasing curve with increasing pressure. The 3889 line shows a very peculiar functional relationship. The apparently sudden drop in intensity above 50 Torr may possibly be explained by the nitrogen impurity commented on earlier in Section III. The nitrogen line (3914Å) is N_2^+. The energy required to ionize N_2 is 14.5 eV. This added to 3.1 eV = 17,400 3914Å is 17.6 eV, which is roughly equal to the 2^3S metastable state energy of helium (about 19.7 eV, from Fig. 3). It is proposed that as the density of helium atoms in the metastable 2^3S state increases, more are available to transfer their energy to the relatively few nitrogen atoms in the collision chamber. This hypothesis is also indicated by the apparent rise in intensity of the nitrogen line on the photographic plates. No intensity vs pressure measurements were made of the nitrogen line.

V. SUMMARY

There appears to be no simple general functional dependence of emission cross section on pressure. However, similarities do exist in several of the lines which hints that a general relationship may exist.

The only line very dissimilar was the 3889Å line which is hypothesized as being caused by an excitation transfer to the nitrogen impurity.

Improvements in the experimental technique may present a more accurate indication of this dependence. It was pointed out earlier that three of the lines visible by photographic methods were of too low intensity to be studied as a function of pressure. This study needs to be done.

As this paper is being written, steps are being taken to modify the optical apparatus which may render this analysis feasible. A mechanical chopper is to be employed in conjunction with a lock-in frequency amplifier. The signal from the photomultiplier tube will then be alternating current. This will greatly decrease the effect of the dark current, (d.c.) and, it is hoped, will result in permitting analysis of lines of very weak intensity. This increased effective intensity should also permit the use of the regular monochrometer slits which will result in higher wavelength resolution.

Absolute measurements have not been attempted in this paper, as only relative values were required to obtain the general picture of the pressure dependence. This experiment was carried out at

indicated proton energies in the region of 1.6 MeV $\pm$ .10 MeV. This is the energy of the beam prior to penetration of the aluminum foil. The actual collisional energy of the protons will have to be determined prior to any absolute measurements.

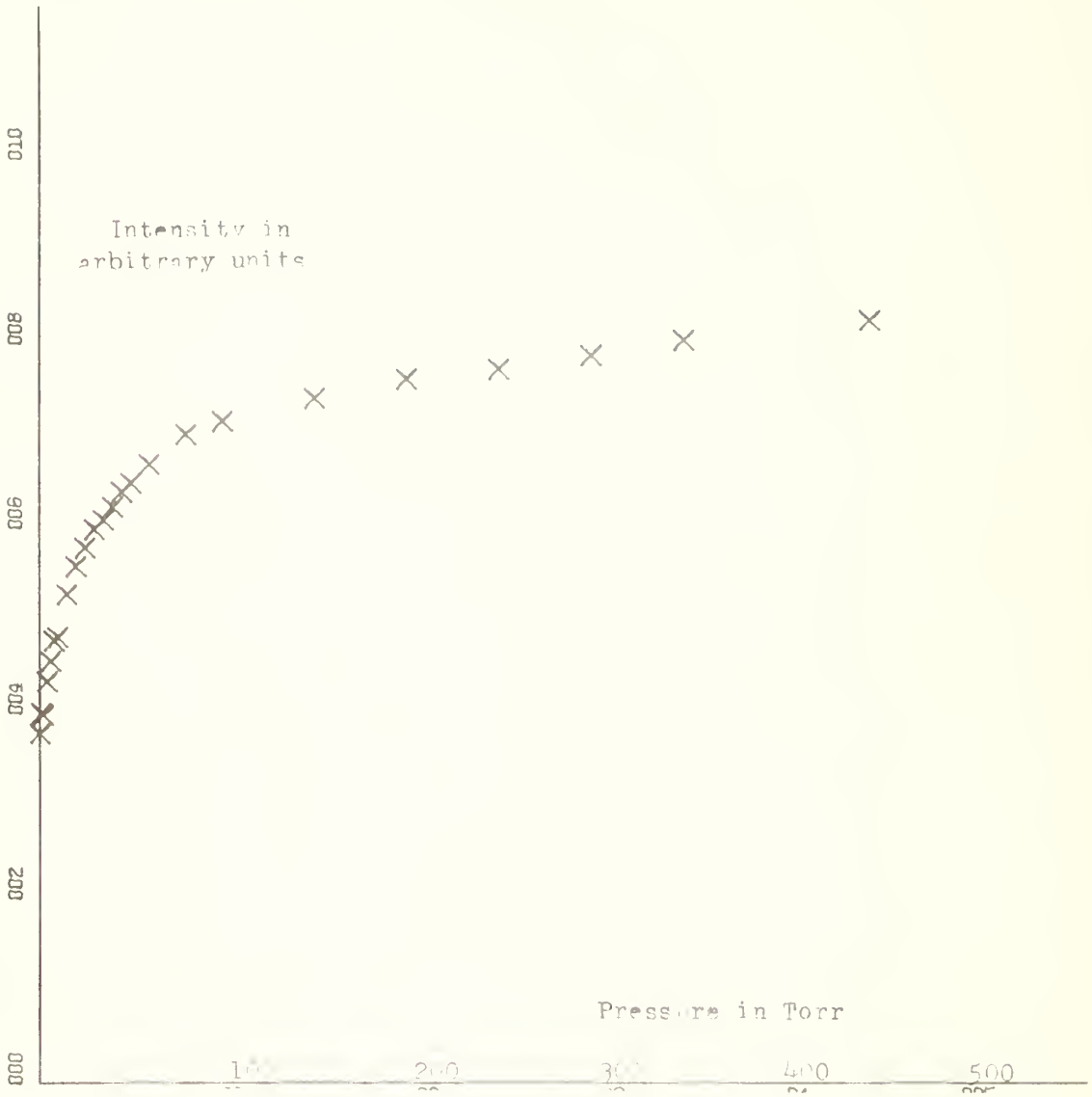

Figure 5. Intensity vs Pressure. 6678Å ($2^1P - 3^1D$) H^+ on Helium.

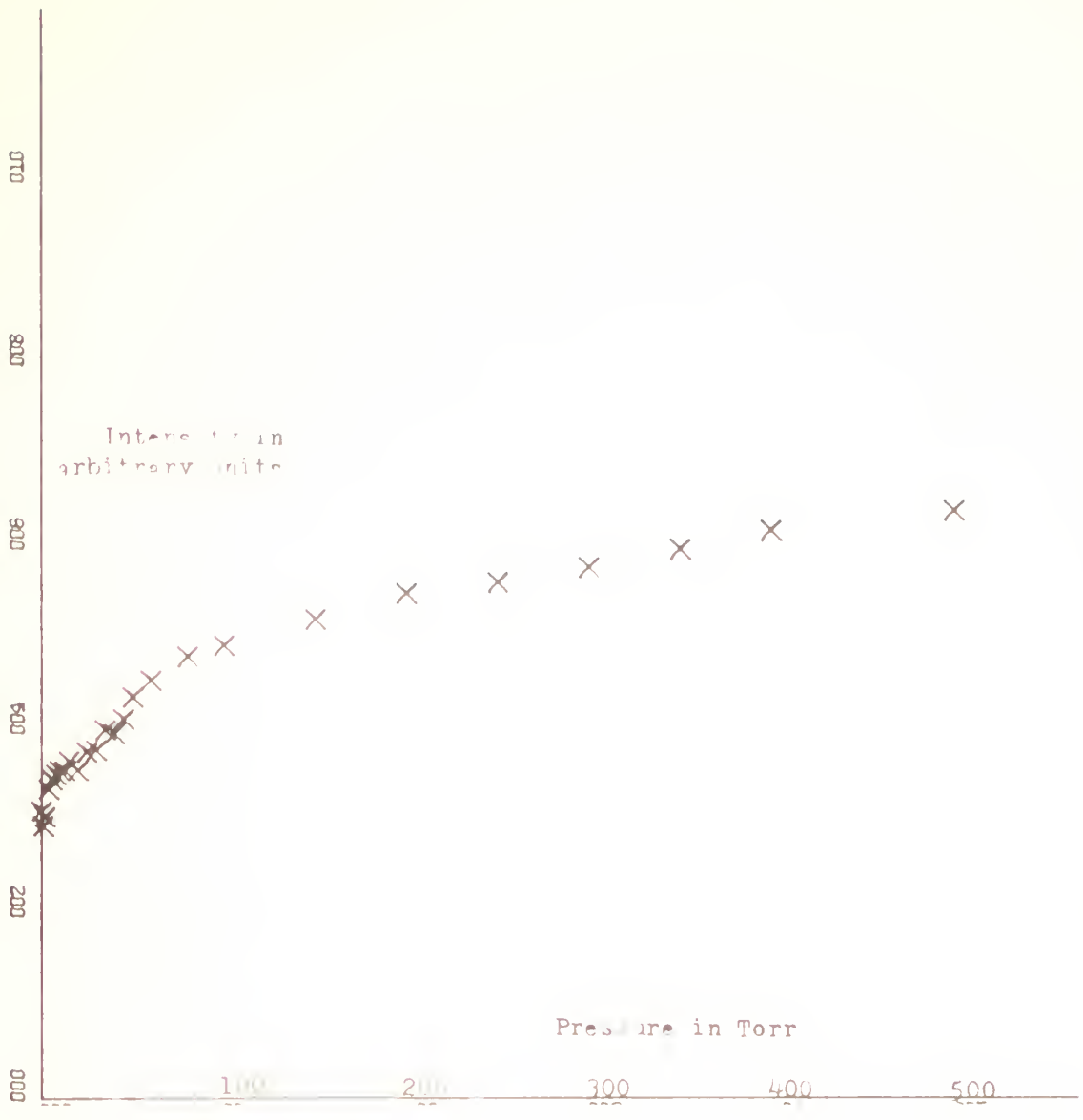

Figure 6. Intensity vs Pressure. 7281Å ($2^1P - 3^1S$) H^+ on Helium.

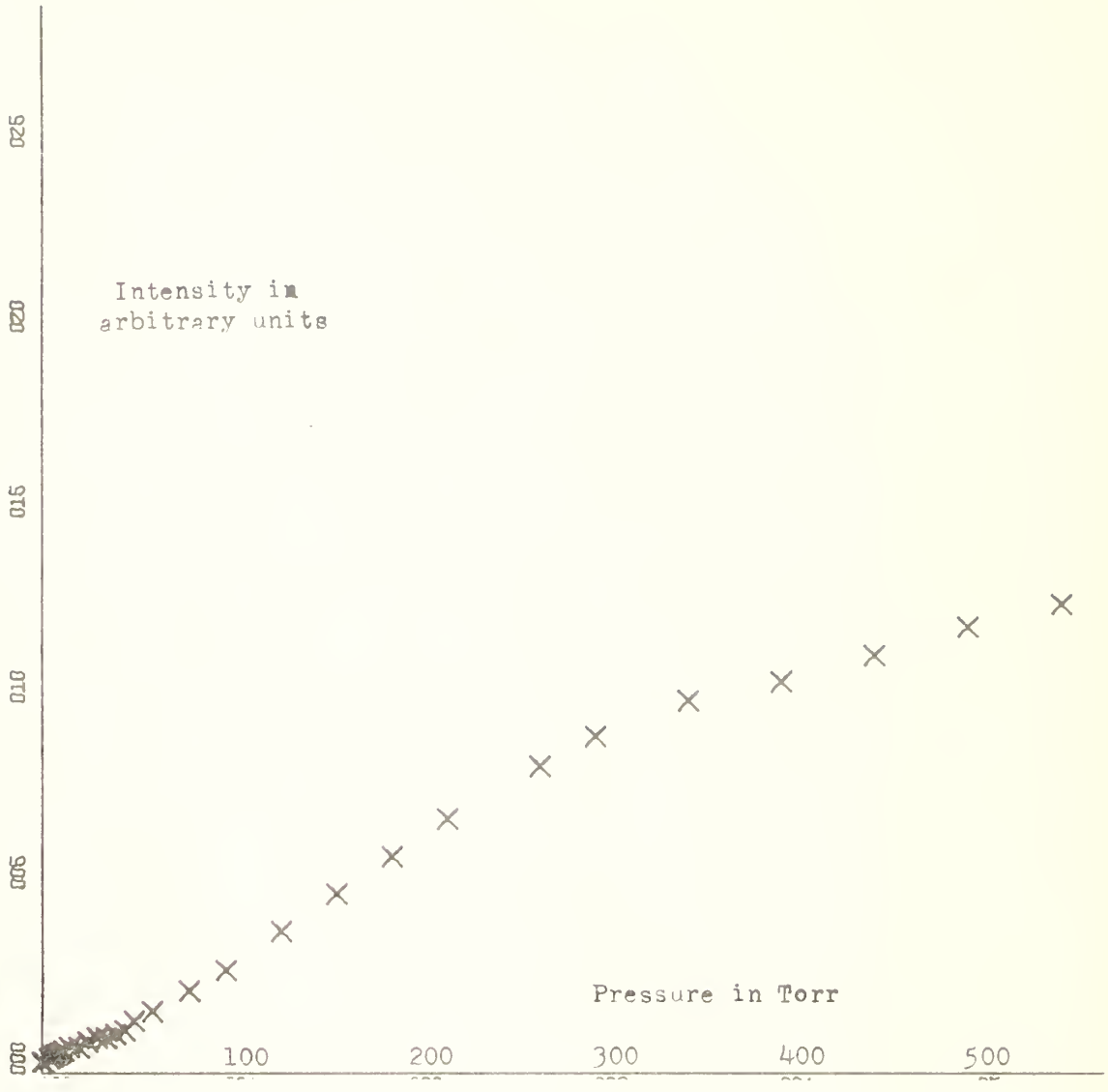

Figure 7. Intensity vs Pressure. 3889Å ($2^3S - 3^3P$). H^+ on Helium.

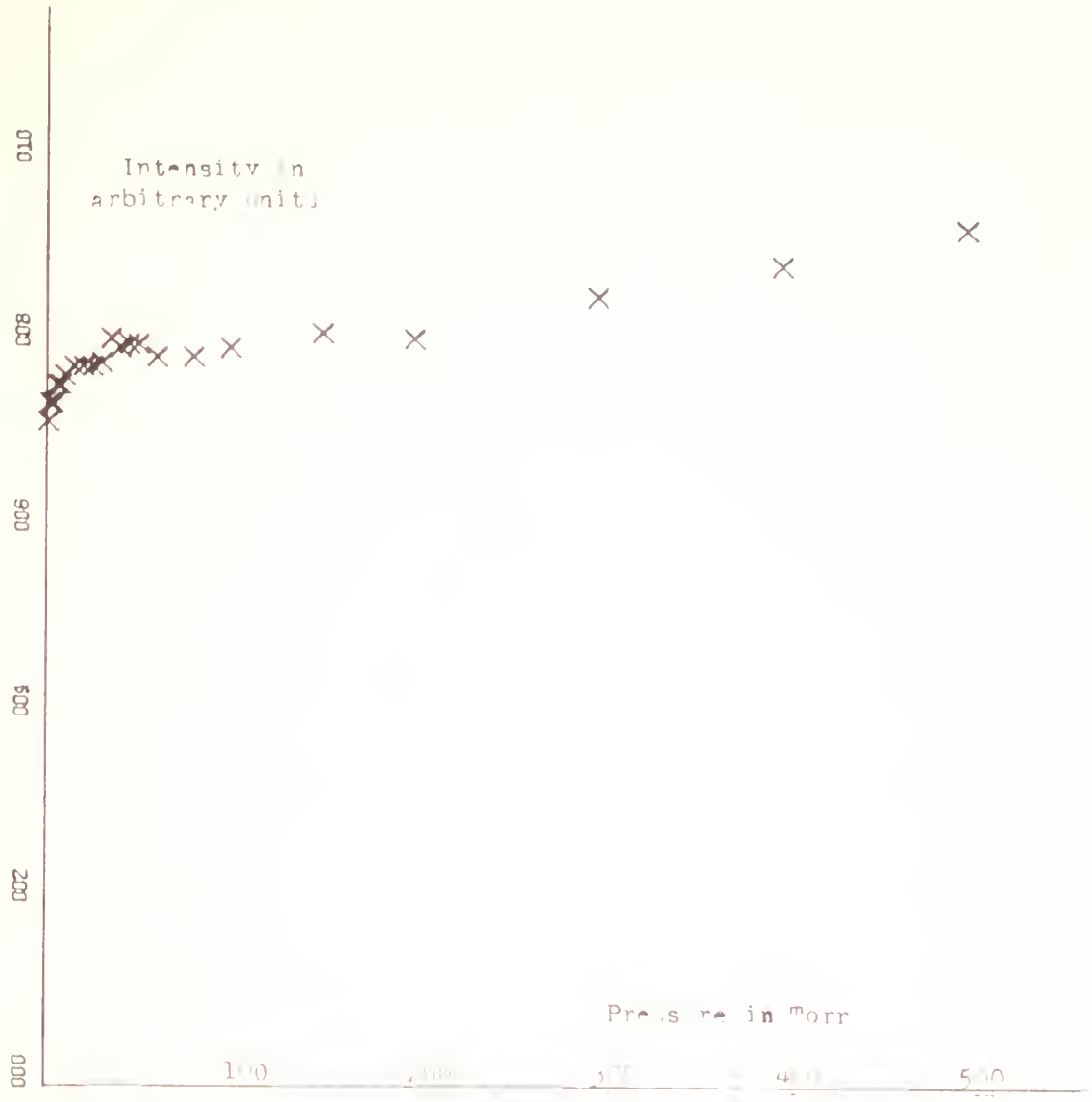

Figure 8. Intensity vs Pressure. 5876Å ($2^3P - 3^3D$). H^+ on Helium.

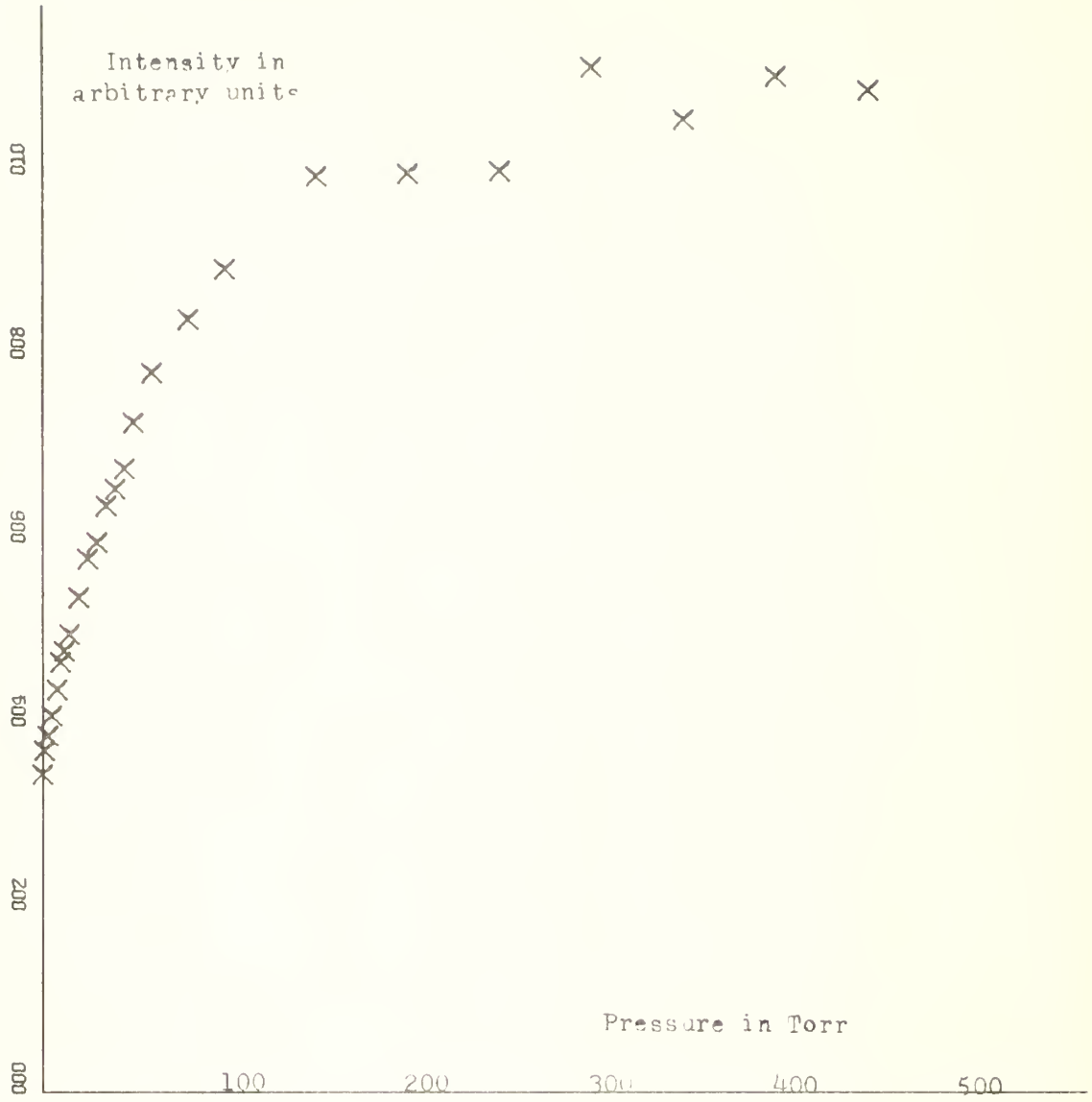

Figure 9. Intensity vs Pressure. 7065Å ($2^3P - 3^3S$). H^+ on Helium.

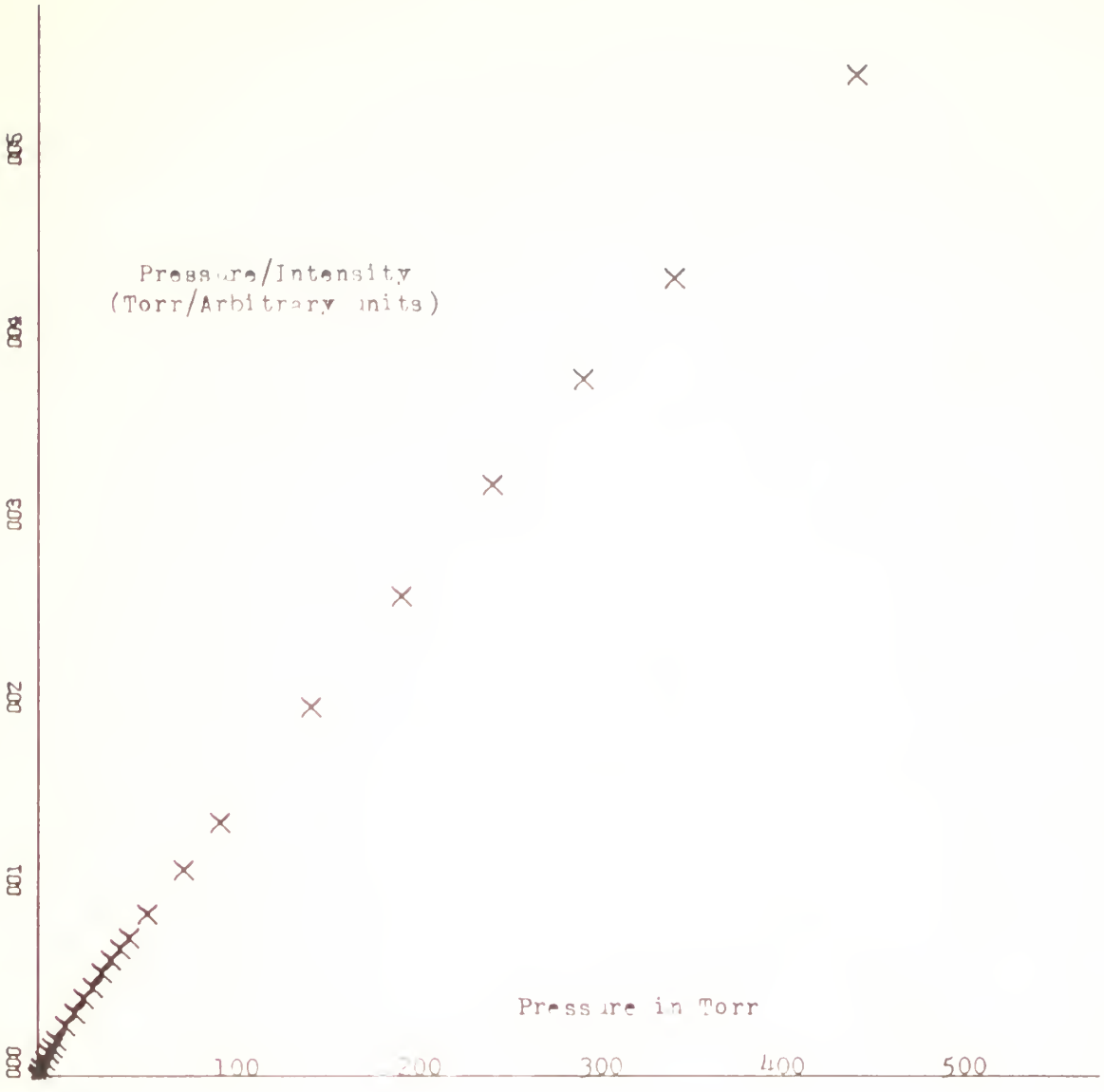

Figure 10. Pressure/Intensity vs Pressure. 6678Å
($2^1P - 3^1D$). H^+ on Helium.

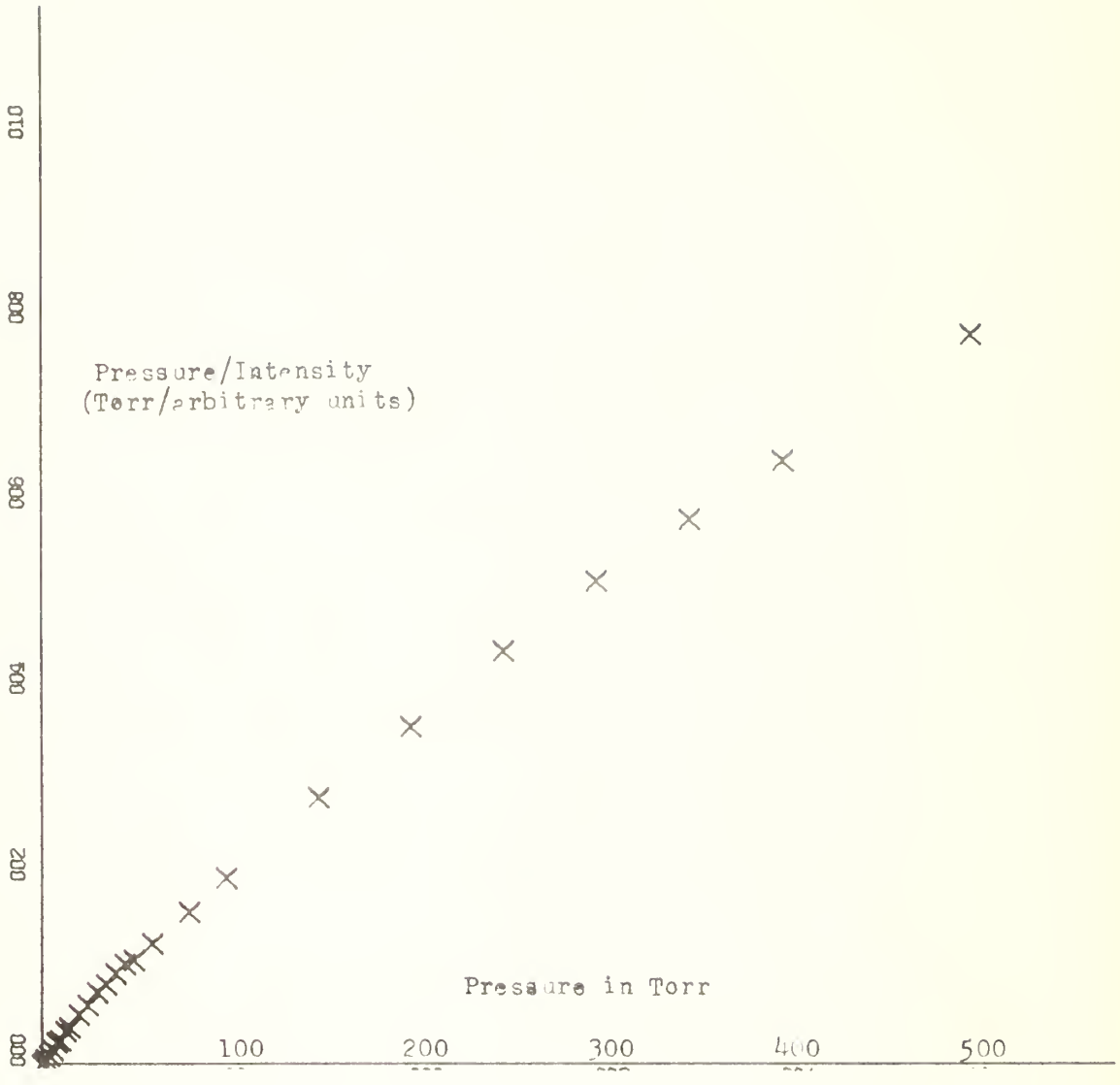

Figure 11. Pressure/Intensity vs Pressure. 7281Å
($2^1P - 3^1S$). H^+ on Helium.

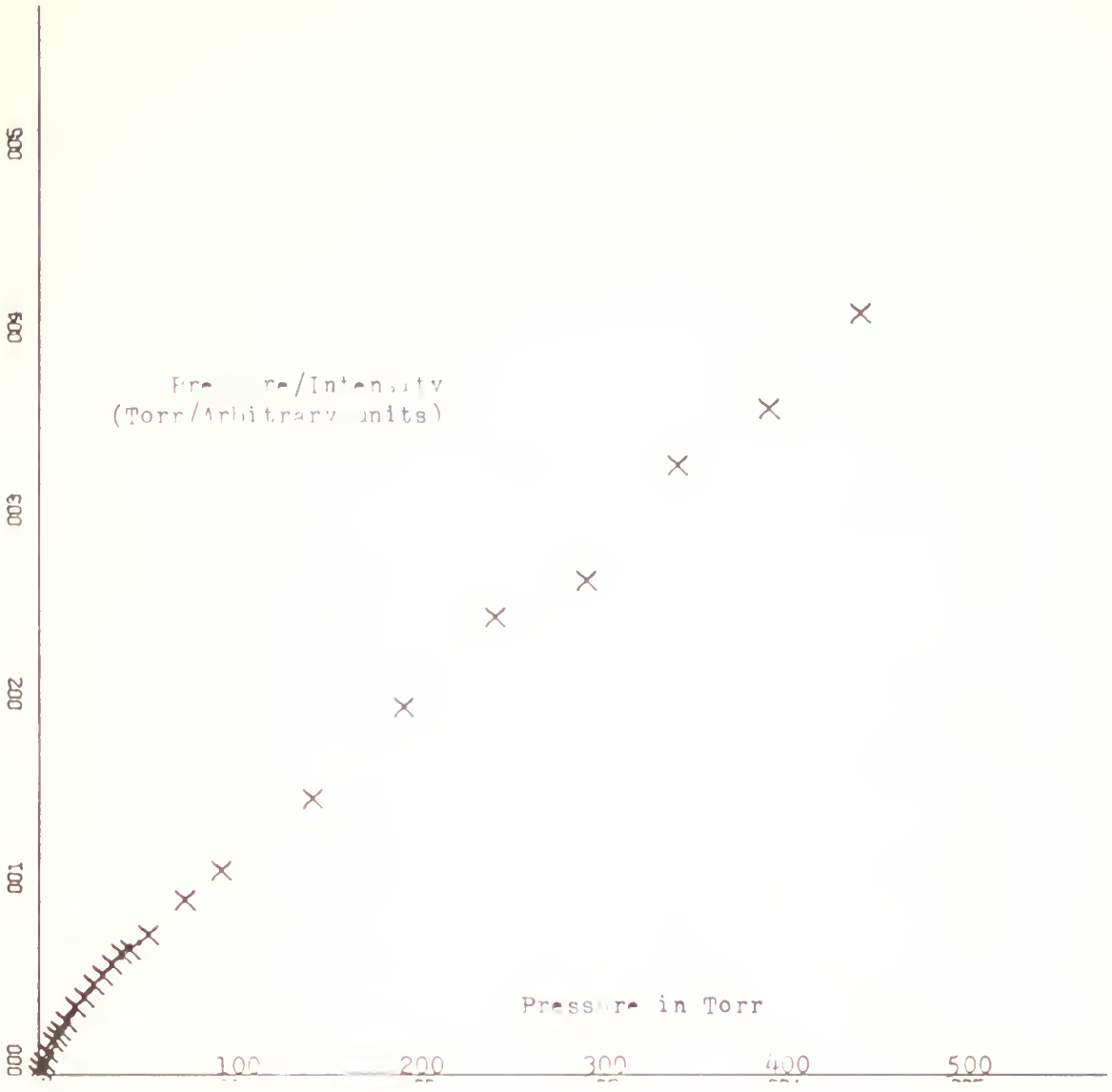

Figure 12. Pressure/Intensity vs Pressure. 7065Å
($2^3P - 3^3S$). H^+ on Helium.

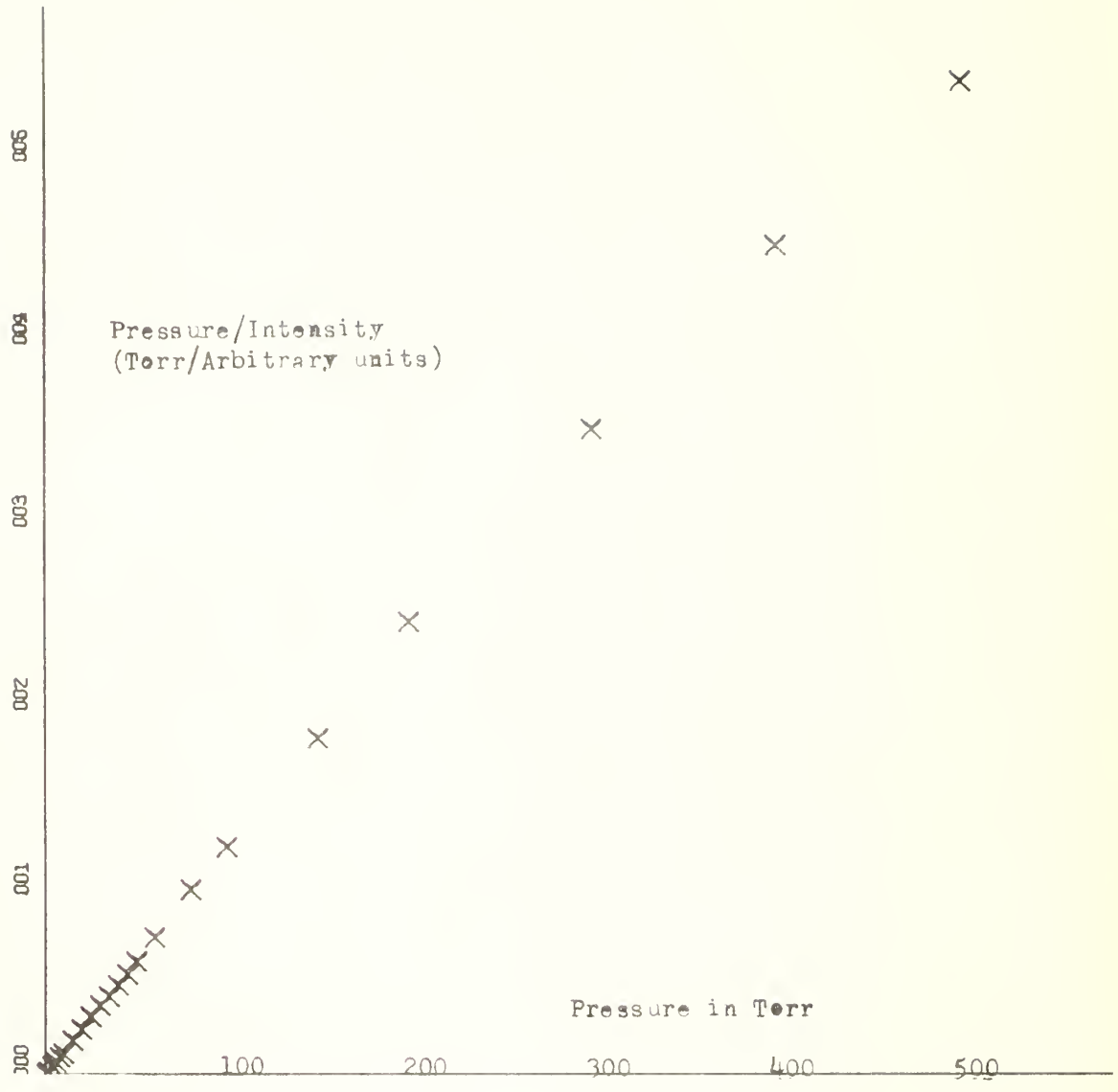

Figure 13. Pressure/Intensity vs Pressure. 5876Å
($2^3P - 3^3D$). H^+ on Helium.

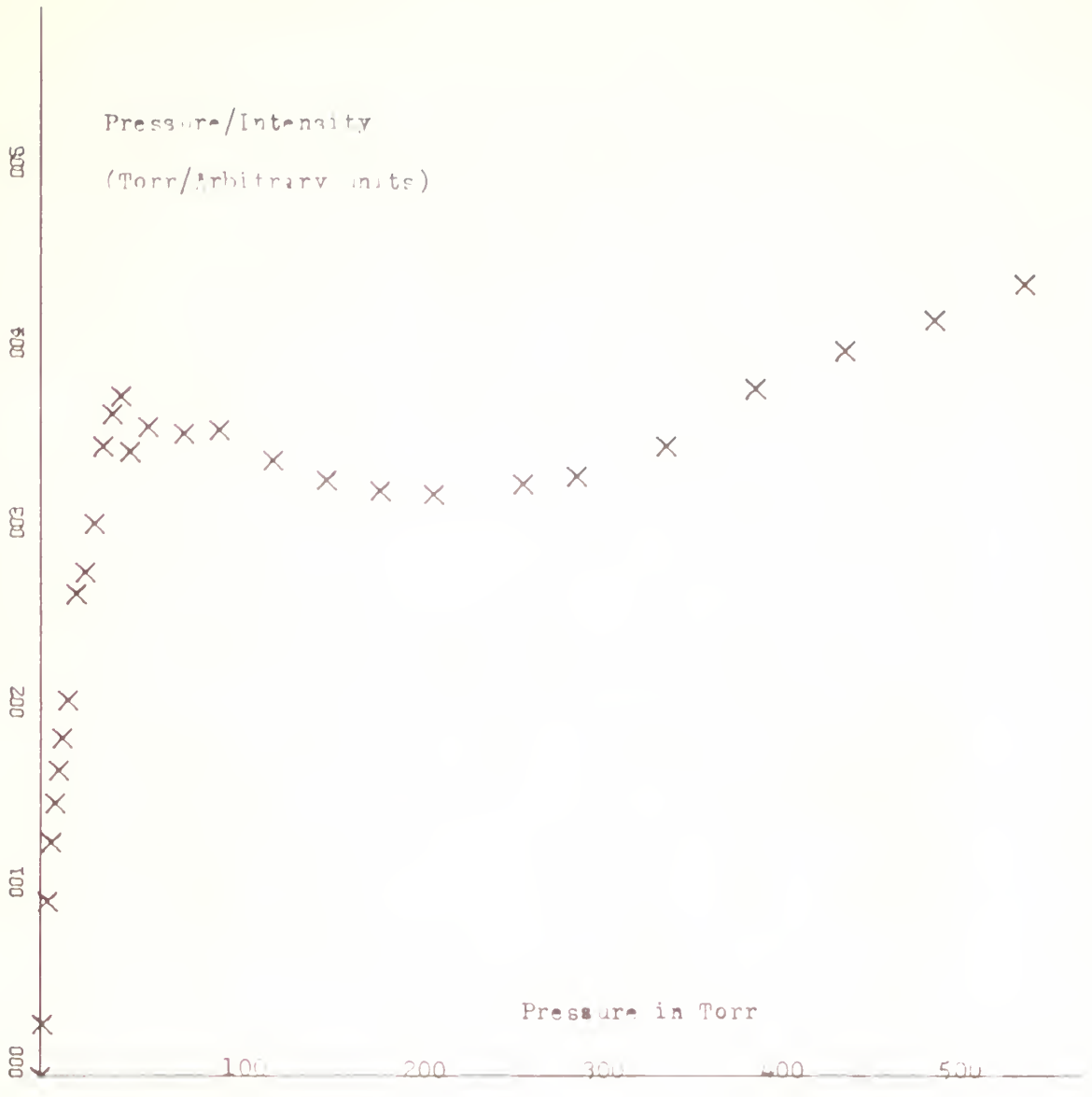

Figure 14. Pressure/Intensity vs Pressure. 3889Å
($2^3S - 3^3P$). H^+ on Helium.

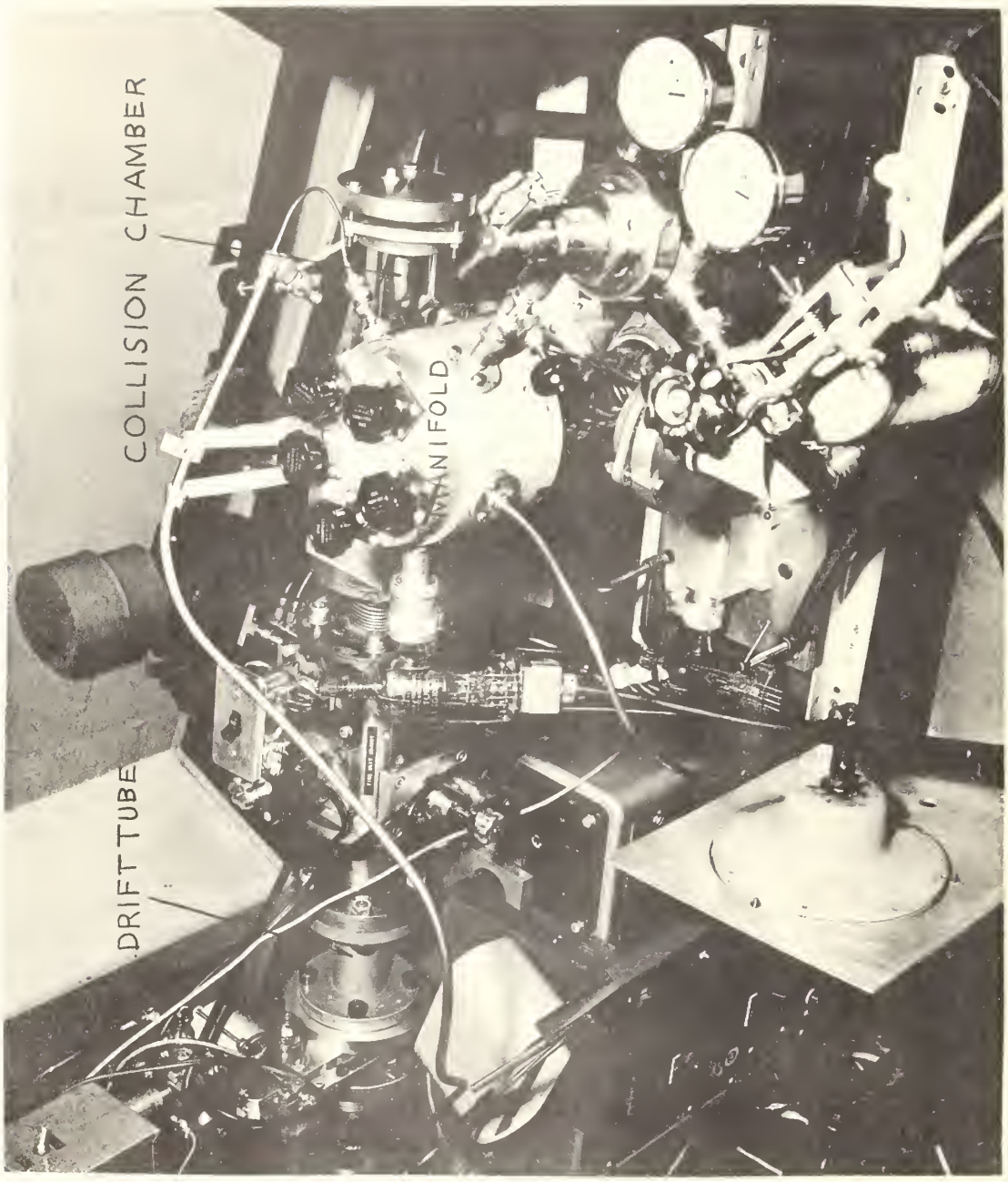

Figure 15. Drift tube, collision chamber and control manifold.

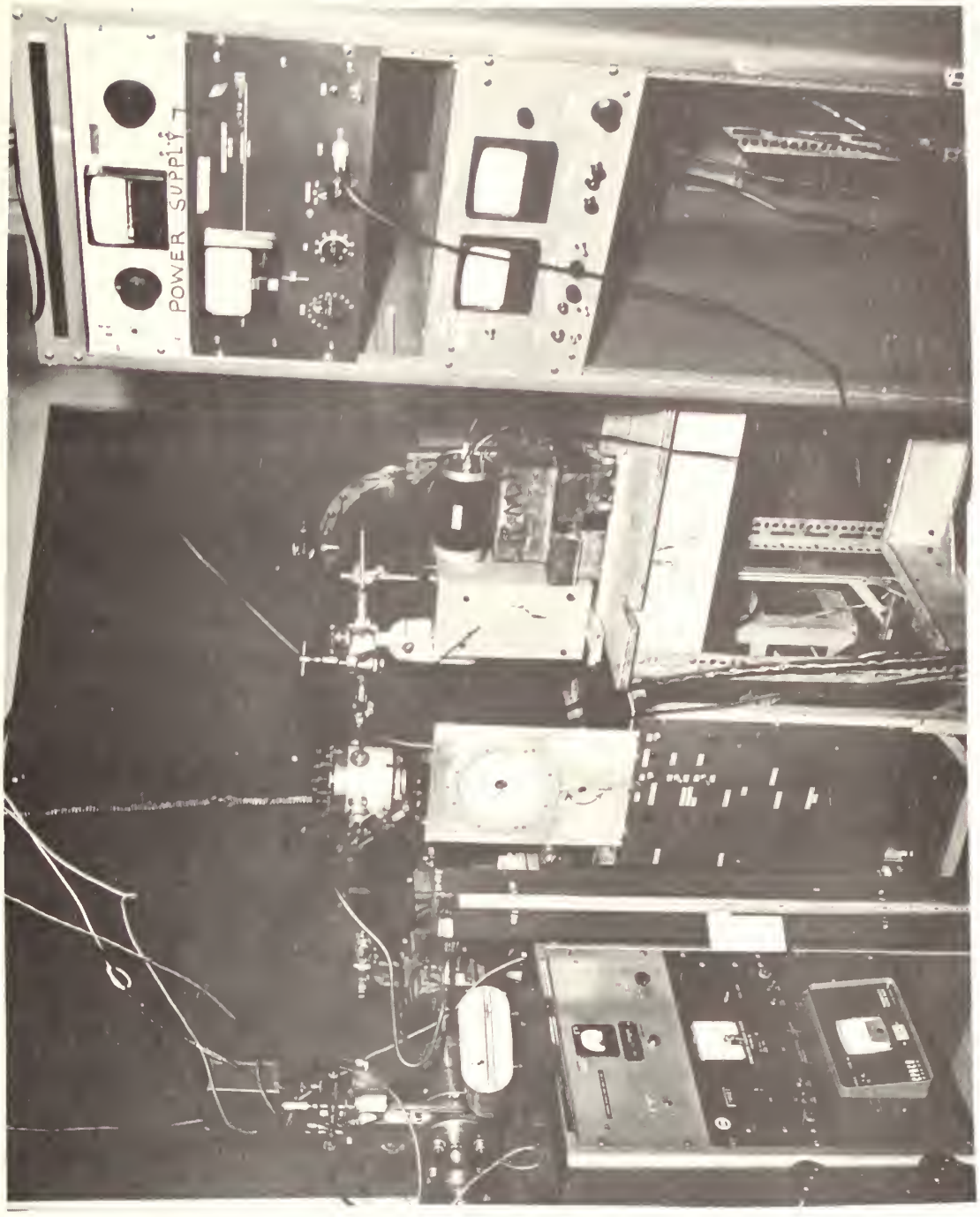

Figure 16. Optical equipment in position.

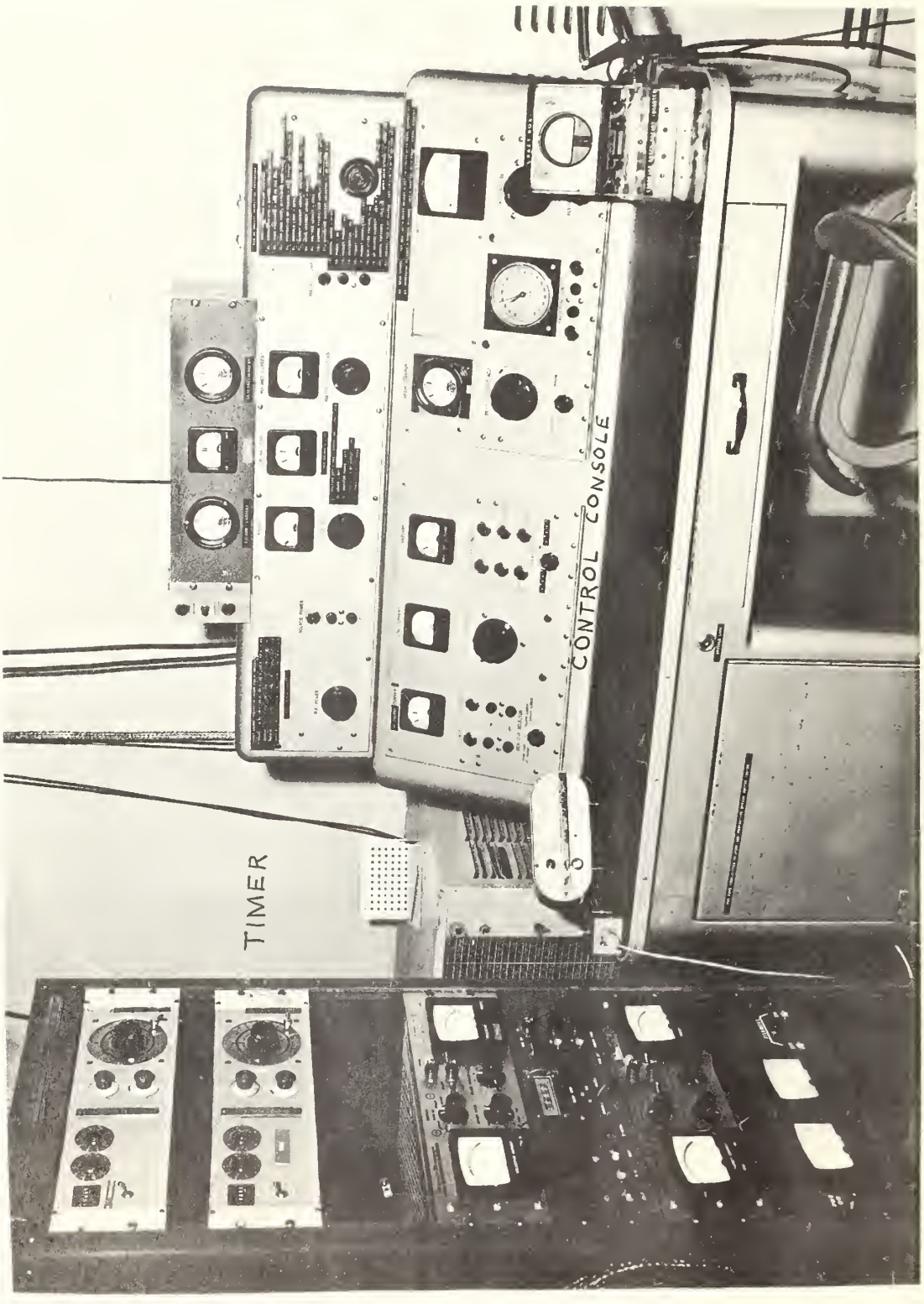

Figure 17. Control console and measuring devices.

BIBLIOGRAPHY

1. Allen, C.W. Astrophysical Quantities. London: The Athlone Press, 1955.

2. De Heer, F.J. "Experimental Studies of Excitation in Collisions between Atomic and Ion Systems", Advances in Atomic and Molecular Physics. D.R. Bater and I. Estermann, editor. Vol. 2 New York: Academic Press, 1966, pp. 328-384.

3. Gabriel, A.H., and D.W.O. Heddle. "Excitation processes in helium", Proceedings of the Royal Society, 258: 124-145, 1960.

4. Hasted, J.B. Physics of Atomic Collisions. London: Butterworth and Co., 1964.

5. Herzberg, G. Molecular Spectra and Molecular Structure. 2nd edition. New York: D. Van Norstrand Company, Inc., 1950.

6. Pearse, R.W.B. and A.G. Gaydon. The Identification of Molecular Spectra. 3rd edition. New York: John Wiley and Son Inc., 1963.

7. Sternberg, Z., and P. Thomas. "Excitation Processes in Helium Induced by Impact of Deuterons and Protons", The Physical Review, 124: 810-813, 1961.

8. Thomas, E.W. "Cross Sections for the Formation of Excited States in a Helium Target by the Impact of 0.15- to 1.0-MeV Protons and Deuterons. II. Comparison with Theory", The Physical Review, 164: 151-155, 1967.

9. Thomas, E.W., and G.D. Bent. "Formation of Excited States in a Helium Target by the Impact of 0.15- to 1.0- MeV Protons and Deuterons, I. Experimental", The Physical Review, 164: 143-150, 1967.

10. Wiese, W.L., M.W. Smith, and B.M. Glennon. Atomic Transition Probabilities Hydrogen Through Neon. National Bureau of Standards, Department of Commerce, Washington: Government Printing Office, 1966.

11. Zaidel, A.N., V.K. Prokof'ev, and S.M. Raiskii. Tables of Spectrum Lines. New York: The Macmillan Company, 1961.

INITIAL DISTRIBUTION LIST

		No. Copies
1.	Defense Documentation Center Cameron Station Alexandria, Virginia 22314	20
2.	Library Naval Postgraduate School Monterey, California 93940	2
3.	Deputy Chief of Staff for Personnel Office of Personnel Operations Department of the Army Washington, D.C. 20310	1
4.	Prof. E.A. Milne Department of Physics Naval Postgraduate School Monterey, California 93940	25
5.	Prof. R.L. Kelly Department of Physics Naval Postgraduate School Monterey, California 93940	1
6.	Maj. B.J. Tullington, Jr. 107 E. Virginia Avenue Hampton, Virginia 23363	2
7.	Defense Atomic Support Agency Department of Defense Washington, D.C. 20301	1

DOCUMENT CONTROL DATA - R & D

(Security classification of title, body of abstract and indexing annotation must be entered when the overall report is classified)

1. ORIGINATING ACTIVITY (Corporate author)

Naval Postgraduate School
Monterey, California 93940

2a. REPORT SECURITY CLASSIFICATION

UNCLASSIFIED

2b. GROUP

3. REPORT TITLE

The Excitation of Helium by High Energy Proton Bombardment at Various Pressures

4. DESCRIPTIVE NOTES (Type of report and inclusive dates)

Thesis, MS, June 1968

5. AUTHOR(S) (First name, middle initial, last name)

Tullington, Bernard J., Jr., MAJ, USA

6. REPORT DATE	7a. TOTAL NO. OF PAGES	7b. NO. OF REFS
June 1968	41	11

8a. CONTRACT OR GRANT NO	9a. ORIGINATOR'S REPORT NUMBER(S)
N/A	N/A
b. PROJECT NO	
c.	9b. OTHER REPORT NO(S) (Any other numbers that may be assigned this report)
d.	N/A

10. DISTRIBUTION STATEMENT

[redacted]

11. SUPPLEMENTARY NOTES	12. SPONSORING MILITARY ACTIVITY
N/A	Naval Postgraduate School

13. ABSTRACT

The intensities of several helium spectral lines are analyzed for their dependence on pressure. Neutral helium was bombarded by protons, accelerated in a Van de Graaff generator to energies of 1.6 MeV before they passed through an aluminum foil window into the collision chamber. Eight helium emission lines and one nitrogen line (impurity) were detected by photographic analysis of the collision spectrum at various pressures. Relative intensities of five of the helium emission lines were measured with photoelectric apparatus at pressures from 10^{-5} - 550 Torr. Lines of 6678Å, 7281Å, 7065Å and 5876Å show a similiar, but not exact, functional dependence on pressure. The 3889Å line appears to have a quite different pressure dependence thay may possibly be due to the nitrogen impurity. Suggested experimental improvements are discussed.

14 KEY WORDS	LINK A		LINK B		LINK C	
	ROLE	WT	ROLE	WT	ROLE	WT
Emission cross section						
Emission function						
Emission intensity						
Excitation cross section						
Single hit condition						

$A_{eq} = \frac{E}{A} \frac{RI}{TC}$